Statistical Mechanical Calculation of Anisotropic Step Stiffness of a Two-Dimensional Hexagonal Lattice Gas Model with Next-Nearest-Neighbor Interactions: Application to Si(111) Surface

Noriko Akutsu[1] and Yasuhiro Akutsu[2]

[1]*Faculty of Engineering, Osaka Electro-Communication University, Hatsu-cho, Neyagawa, Osaka 572, Japan*
[2]*Department of Physics, Graduate School of Science, Osaka University, Machikaneyama-cho, Toyonaka, Osaka 560, Japan*

(July 31, 2018)

We study a two-dimensional honeycomb lattice gas model with both nearest- and next-nearest-neighbor interactions in a staggered field, which describes the surface of stoichiometrically binary crystal. We calculate anisotropic step tension, step stiffness, and equilibrium island shape, by an extended random walk method. We apply the results to Si(111) 7×7 reconstructed surface and high-temperature Si(111) 1×1 surface. We also calculate inter-step interaction coefficient.

PACS numbers: 68.35.Md, 68.35.-p, 50.50.+q, 64.60.-i

I. INTRODUCTION

Recent developments of the experimental techniques such as STM (scanning-tunneling microscopy) [1], LEEM (low-energy electron microscopy) [2] and REM (reflection electron microscopy) [3] make it possible to observe a step on a crystal surface in the wide range of the length scales. However, the connection among quantities measured in different scales has not been clarified yet.

In Ref. [4], for two-dimensional (2D) square-lattice Ising model with both nearest- and next-nearest-neighbor (nn and nnn) interactions, we calculated anisotropic interface tension and interface stiffness by the imaginary path-weight (IPW) method which is an extended Feynman-Vdovichenko's random walk method [5–8]. In the method, the overhang structure in a step is taken into account, which leads to high accuracy of the results in a wide range of temperature.

We applied the results to Si(001) surface based on the microscopic kink energy obtained by the Swartzentruber *et al.* [9]. The Ising result gave a satisfactory explanation for experimentally measured step tension γ, step stiffness $\tilde{\gamma}$ and equilibrium island shape obtained by Bartel t *et al.* [10] on Si(001) surface.

In the present paper, we consider the honeycomb lattice Ising system in a staggered field, with both nn and nnn interactions, to calculate interface tension, interface stiffness, island shape and the coefficient of step interaction by the IPW method. We aim at applying the results to Si(111) 7×7 reconstructed surfaces and high-temperature Si(111) 1×1 surface.

II. MODEL HAMILTONIAN

We consider a honeycomb lattice with $2N$ sites. We decompose the lattice into two triangular sublattices designated by A and B. On the A-sublattice, we define the occupation variable C_{Ai} which takes 1 (present) or 0 (absent) at the site i. Similarly, we define C_{Bj} for the B-sublattice.

The lattice gas Hamiltonian $\mathcal{H}_{LG}$ is then written as

$$\mathcal{H}_{LG} = -4J_1 \sum_{<i,j>} [C_{Ai}C_{Bj} - \frac{1}{2}(C_{Ai} + C_{Bj})]$$

$$-4J_{A2} \sum_{<i,j>} [C_{Ai}C_{Aj} - \frac{1}{2}(C_{Ai} + C_{Aj})]$$

$$-4J_{B2} \sum_{<i,j>} [C_{Bi}C_{Bj} - \frac{1}{2}(C_{Bi} + C_{Bj})]$$

$$-\epsilon_A \sum_{i=1}^{N} C_{Ai} - \epsilon_B \sum_{i=1}^{N} C_{Bi}, \qquad (2.1)$$

where $4J_1$ is the bond energy between A-atom and B-atom of the nn sites, $4J_{A2}$ and $4J_{B2}$ are the bond energies between nnn atoms. $\epsilon_A(\epsilon_B)$ is the "surface chemical potential" of A-atom (B-atom). We consider the simplest case where ϵ_A and ϵ_B are given by

$$\left. \begin{array}{l} \epsilon_A = \mu_{A,gas}(P_A, P_B, T) - \mu_{A,surf}(T), \\ \epsilon_B = \mu_{B,gas}(P_A, P_B, T) - \mu_{B,surf}(T). \end{array} \right\} \qquad (2.2)$$

In the above, $\mu_{A,gas}(P_A, P_B, T)$ is the chemical potential of A-atom in the gas, P_A is the partial pressure of A-atom in the gas phase (similarly for $\mu_{B,solid}(T)$, $\mu_{B,gas}(P_A, P_B, T)$ and P_B); $\mu_{A,surf}(T)$ and $\mu_{B,surf}(T)$ are expressed as

$$\begin{array}{l} \mu_{A,surf} = \Delta E(T) + \mu_{solid}(T), \\ \mu_{B,surf} = -\Delta E(T) + \mu_{solid}(T), \end{array} \qquad (2.3)$$

where $\Delta E(T)$ has been introduced as the difference from the chemical potential of atoms in the bulk solid $\mu_{solid}(T)$.

Let us consider the bulk phase-coexistence state of the stoichiometrically binary system. Total chemical potential of the system has to be unchanged under removal of one pair of AB atoms from crystal into vapor and vice-versa. Hence, as the coexistence condition, we have

$$\mu_{\mathrm{A,gas}}(P_{\mathrm{A}}, P_{\mathrm{B}}, T) + \mu_{\mathrm{B,gas}}(P_{\mathrm{A}}, P_{\mathrm{B}}, T)$$
$$= 2\mu_{\mathrm{solid}}(T). \qquad (2.4)$$

Combining (2.2)– (2.4), we obtain

$$\epsilon_{\mathrm{B}} = -\epsilon_{\mathrm{A}}. \qquad (2.5)$$

This condition also means that, in the lattice gas Hamiltonian (2.1), the total energy of the all-occupied state is the same at that of the all-empty state.

Let us introduce the Ising spin variables $\{\sigma_{\mathrm{A}i}\}$ and $\{\sigma_{\mathrm{B}i}\}$ as

$$\sigma_{\mathrm{A}i} = 2\left(C_{\mathrm{A}i} - \frac{1}{2}\right), \quad \sigma_{\mathrm{B}i} = 2\left(\frac{1}{2} - C_{\mathrm{B}i}\right). \qquad (2.6)$$

Substituting (2.6) into the Hamiltonian (2.1) together with (2.5), we have the Ising AF Hamiltonian $\mathcal{H}$:

$$\begin{aligned}
\mathcal{H} &= \mathcal{H}_{\mathrm{LG}} + Nz_6 J_1 + Nz_3(J_{\mathrm{A}2} + J_{\mathrm{B}2})/2, \\
&= J_1 \sum_{<i,j>} \sigma_{\mathrm{A}i}\sigma_{\mathrm{B}j} - J_{\mathrm{A}2} \sum_{<i,j>} \sigma_{\mathrm{A}i}\sigma_{\mathrm{A}j} \\
&\quad - J_{\mathrm{B}2} \sum_{<i,j>} \sigma_{\mathrm{B}i}\sigma_{\mathrm{B}j} - H \sum_{i=1}^{N} \sigma_{\mathrm{A}i} - H \sum_{i=1}^{N} \sigma_{\mathrm{B}i} \\
&\quad + Nz_6 J_1 + Nz_3(J_{\mathrm{A}2} + J_{\mathrm{B}2})/2, \\
H &= \epsilon_{\mathrm{A}}/2 \qquad (2.7)
\end{aligned}$$

where $z_6 = 3$ and $z_3 = 6$ are the coordination numbers of honeycomb lattice and triangular lattice, respectively.

III. IMAGINARY PATH-WEIGHT METHOD

We calculate interface quantities by a random walk method with imaginary path-weight(IPW) [6–8]. We regard an interface with zigzag configuration as a trace of 2D *free* random walk.

Consider an interface which connects site O and P. We denote the distance between site O and P by R (Fig. 1). The interface of the two-dimensional Ising model is made by fixing the boundary spins as depicted in Fig. 1. Let us denote the partition function the Ising model with and without interface by $Z_R^{+-}(\theta)$ and Z_R^{++}, respectively, where θ is the slant angle of an interface relative to a lattice axis. [11,12] The interface tension $\gamma(\theta, T)$ is defined as

$$\gamma(\theta, T) = -k_{\mathrm{B}}T \lim_{R \to \infty} \frac{1}{R} \ln\left[\frac{Z_R^{+-}(\theta)}{Z_R^{++}}\right], \qquad (3.1)$$

where $Z_R^{+-}(\theta)/Z_R^{++}$ is regarded as the interface partition function $\mathcal{G}$.

We apply Vdovichenko's method [5] to deal with the low-temperature diagrammatic expansion of $Z_R^{+-}(\theta)$ and Z_R^{++}. The method, which originally treated the high-temperature expansion of the partition function,

also works for low-temperature expansion to evaluate weighted sum over all possible domain-wall configurations. The essential point in the Vdovichenko's method is introduction of the imaginary factor $e^{i\phi/2}$ at each turn (with angle ϕ) of the random walks of the domain wall. With this simple recipe, the problem reduces to a free random walk problem on a lattice.

We see that Z_R^{++} equals weighted sum over possible configurations of closed domain walls; and $Z_R^{+-}(\theta)$ equals weighted sum over possible configurations of closed domain walls plus a single "open" domain wall traversing the lattice. In evaluating $Z_R^{+-}(\theta)$ by Vdovichenko's method, the free random walk nature allows us to "decouple" the open domain wall from closed domain walls. [6,7] Therefore, in the limit of $R \to \infty$, the interface partition function is equivalent to the "edge-to-edge" lattice Green's function of the free random walk with running on the dual lattice. [7] Thus, in the limit of $R \to \infty$, the interface partition function $\mathcal{G}$ is written as [7]

$$\begin{aligned}
\mathcal{G} &= \exp(-\gamma(\theta)R/k_{\mathrm{B}}T) \\
&= \frac{1}{(2\pi)^2} \int_{-\pi}^{\pi} \int_{-\pi}^{\pi} dk_x dk_y \frac{e^{i\boldsymbol{k}\boldsymbol{R}}}{D(\boldsymbol{k})}, \qquad (3.2)
\end{aligned}$$

where the D-function is defined as

$$D(\boldsymbol{k}) = \det[1 - \hat{A}(\boldsymbol{k})]. \qquad (3.3)$$

Here, $\hat{A}(\boldsymbol{k})$ is the Fourier component of the connectivity matrix $A(\boldsymbol{r})$ which characterizes the random walk.

The above-described imaginary path-weight random walk method to calculate $\gamma(\theta, T)$ is exact only for solvable cases. However, we have verified that the method works fairly well also for non-solvable cases [4,8,13,14].

After evaluating the integral by the pure imaginary saddle point $\boldsymbol{\omega} = (\omega_x, \omega_y)$, we obtain a set of equations as

$$\begin{aligned}
D(i\boldsymbol{\omega}) &= 0, \\
\frac{\partial D(i\boldsymbol{\omega})}{\partial \omega_y} \Big/ \frac{\partial D(i\boldsymbol{\omega})}{\partial \omega_x} &= \tan\theta, \qquad (3.4)
\end{aligned}$$

and

$$\gamma(\theta, T) = k_{\mathrm{B}}T(\omega_x \cos\theta + \omega_y \sin\theta). \qquad (3.5)$$

From the thermodynamical theory on equilibrium crystal shape(island shape) [16], we have,

$$\omega_x = \lambda y/k_{\mathrm{B}}T, \qquad \omega_y = \lambda x/k_{\mathrm{B}}T, \qquad (3.6)$$

where λ is the Lagrange multiplier associated with the volume-fixing constraint in the Wulff construction, and x and y are the Cartesian coordinates describing the 2D island shape. Thus, we obtain the island shape directly from (3.4) with (3.5). Eq. (3.6) gives relation between the interface orientation angle θ and the point (x, y) on the island shape.

The interface stiffness, which we denote by $\tilde{\gamma}(\theta)$, is given by [13]

$$\tilde{\gamma}(\theta) = \gamma(\theta) + \frac{\partial^2 \gamma(\theta)}{\partial \theta^2}$$
$$= k_{\mathrm{B}}T\sqrt{D_x^2 + D_y^2} \cdot [-D_{xx}\sin^2\theta$$
$$+ D_{xy}\sin 2\theta - D_{yy}\cos^2\theta]^{-1}, \qquad (3.7)$$

where

$$D_x = \frac{\partial D}{\partial \omega_x}, \quad D_y = \frac{\partial D}{\partial \omega_x},$$

$$D_{xx} = \frac{\partial^2 D}{\partial \omega_x^2}, \quad D_{yy} = \frac{\partial^2 D}{\partial \omega_y^2},$$

$$D_{xy} = n\frac{\partial^2 D}{\partial \omega_x \omega_y}. \qquad (3.8)$$

The one-dimensional interface of the lattice gas corresponds to a step on the vicinal surface. For the vicinal surfaces, the surface free energy per projected area, which we denote by $f(\rho)$, is written as [17–19]

$$f(\rho) = f(0) + \gamma(\theta)\rho + B(\theta)\rho^3,$$
$$\rho = \frac{1}{a_h}\tan\phi, \qquad (3.9)$$

where ρ is the step density, ϕ is the tilted angle of the vicinal surface, and a_h is the step height, and $B(\theta)$ is the inter-step interaction coefficient. We have [20,21]

$$B(\theta) = \frac{\pi^2}{6}\frac{(k_{\mathrm{B}}T)^2}{\tilde{\gamma}(\theta)}\lambda^2(g_0),$$

$$\lambda(g_0) = \frac{1}{2}\left(1 + \sqrt{1 + \frac{4\tilde{\gamma}(\theta)}{(k_{\mathrm{B}}T)^2}g_0}\right). \qquad (3.10)$$

where g_0 is the coupling constant of the long range interaction between the steps of the form g_0/r_s^2 (r_s is the step separation distance). Note that, in the limit of $g_0 \to 0$, the factor $\lambda(g)$ approaches unity, leading to [18,19]

$$B(\theta) = \frac{\pi^2}{6}\frac{(k_{\mathrm{B}}T)^2}{\tilde{\gamma}(\theta)}. \qquad (3.11)$$

Hence, the stiffness (3.7) can be utilized in determining the inter-step interaction coefficient $B(\theta)$.

IV. THE CONNECTIVITY MATRIX AND THE D–FUNCTION

A. The honeycomb lattice gas model with next nearest neighbor interaction

We apply the IPW method to calculate interface quantities of the nnn Ising model on the honeycomb lattice described by Hamiltonian (2.1,2.7) (Fig. 2). The Fourier components of the connectivity matrix $(A_{m,n})$ are

$$A_{1,1} = \exp(\mathrm{i}k_x)W/W_H,$$
$$A_{2,1} = \exp(\mathrm{i}k_x)W/W_H r_p,$$
$$A_{3,1} = \exp(\mathrm{i}k_x)W/W_H r_p r_p W_a,$$
$$A_{5,1} = \exp(\mathrm{i}k_x)W/W_H r_m r_m W_b,$$
$$A_{6,1} = \exp(\mathrm{i}k_x)W/W_H r_m,$$
$$A_{1,2} = \exp(\mathrm{i}k_x/2 + \mathrm{i}k_y c_y)W \cdot W_H r_m,$$
$$A_{2,2} = \exp(\mathrm{i}k_x/2 + \mathrm{i}k_y c_y)W \cdot W_H,$$
$$A_{3,2} = \exp(\mathrm{i}k_x/2 + \mathrm{i}k_y c_y)W \cdot W_H r_p,$$
$$A_{4,2} = \exp(\mathrm{i}k_x/2 + \mathrm{i}k_y c_y)W \cdot W_H r_p r_p W_b,$$
$$A_{6,2} = \exp(\mathrm{i}k_x/2 + \mathrm{i}k_y c_y)W \cdot W_H r_m r_m W_a,$$
$$A_{1,3} = \exp(-\mathrm{i}k_x/2 + \mathrm{i}k_y c_y)W/W_H r_m r_m W_b,$$
$$A_{2,3} = \exp(-\mathrm{i}k_x/2 + \mathrm{i}k_y c_y)W/W_H r_m,$$
$$A_{3,3} = \exp(-\mathrm{i}k_x/2 + \mathrm{i}k_y c_y)W/W_H,$$
$$A_{4,3} = \exp(-\mathrm{i}k_x/2 + \mathrm{i}k_y c_y)W/W_H r_p,$$
$$A_{5,3} = \exp(-\mathrm{i}k_x/2 + \mathrm{i}k_y c_y)W/W_H r_p r_p W_a,$$
$$A_{2,4} = \exp(-\mathrm{i}k_x)W \cdot W_H r_m r_m W_a,$$
$$A_{3,4} = \exp(-\mathrm{i}k_x)W \cdot W_H r_m,$$
$$A_{4,4} = \exp(-\mathrm{i}k_x)W \cdot W_H,$$
$$A_{5,4} = \exp(-\mathrm{i}k_x)W \cdot W_H r_p,$$
$$A_{6,4} = \exp(-\mathrm{i}k_x)W \cdot W_H r_p r_p W_b,$$
$$A_{1,5} = \exp(-\mathrm{i}k_x/2 - \mathrm{i}k_y c_y)W/W_H r_p r_p W_a,$$
$$A_{3,5} = \exp(-\mathrm{i}k_x/2 - \mathrm{i}k_y c_y)W/W_H r_m r_m W_b,$$
$$A_{4,5} = \exp(-\mathrm{i}k_x/2 - \mathrm{i}k_y c_y)W/W_H r_m,$$
$$A_{5,5} = \exp(-\mathrm{i}k_x/2 - \mathrm{i}k_y c_y)W/W_H,$$
$$A_{6,5} = \exp(-\mathrm{i}k_x/2 - \mathrm{i}k_y c_y)W/W_H r_p,$$
$$A_{1,6} = \exp(\mathrm{i}k_x/2 - \mathrm{i}k_y c_y)W \cdot W_H r_p,$$
$$A_{2,6} = \exp(\mathrm{i}k_x/2 - \mathrm{i}k_y c_y)W \cdot W_H r_p r_p W_b,$$
$$A_{4,6} = \exp(\mathrm{i}k_x/2 - \mathrm{i}k_y c_y)W \cdot W_H r_m r_m W_a,$$
$$A_{5,6} = \exp(\mathrm{i}k_x/2 - \mathrm{i}k_y c_y)W \cdot W_H r_m,$$
$$A_{6,6} = \exp(\mathrm{i}k_x/2 - \mathrm{i}k_y c_y)W \cdot W_H,$$
$$\text{others} = 0, \qquad (4.1)$$

where $\mathrm{i}^2 = -1$, $c_y = \sqrt{3}/2$, $W = \exp[-2(J_1 + 2J_{\mathrm{A}2} + 2J_{\mathrm{B}2})/(k_{\mathrm{B}}T)]$, $W_H = \exp[-2H/(3k_{\mathrm{B}}T)]$, $W_a = \exp[4J_{\mathrm{A}2}/(k_{\mathrm{B}}T)]$, $W_b = \exp[4J_{\mathrm{B}2}/(k_{\mathrm{B}}T)]$, $r_p = \exp(\mathrm{i}\pi/6)$ and $r_m = \exp(-\mathrm{i}\pi/6)$.

Then, the D-function defined by (3.3) is

$$D(k_x, k_y) = M + c_1 \cosh(k_x) +$$
$$c_1 \cosh(k_x/2 - c_y k_y) + c_1 \cosh(k_x/2 + c_y k_y) +$$
$$c_2 \cosh(2k_x) + c_2 \cosh(k_x - 2c_y k_y) +$$
$$c_2 \cosh(k_x + 2c_y k_y) + c_3 \cosh(2c_y k_y) +$$
$$c_3 \cosh(3k_x/2 - c_y k_y) + c_3 \cosh(3k_x/2 + c_y k_y) +$$
$$s_1 \sinh(k_x) + s_2 \sinh(2k_x) -$$
$$s_2 \sinh(k_x - 2c_y k_y) + s_4 \sinh(k_x/2 - c_y k_y) +$$
$$s_4 \sinh(k_x/2 + c_y k_y) - s_2 \sinh(k_x + 2c_y k_y), \qquad (4.2)$$

3

where

$$M = 1 + 3W^2 + 4W^6 - W^3/W_H^3 - W^3W_H^3 -$$
$$12W^6W_a + 9W^6W_a^2 + 4W^6W_a^3 +$$
$$(W^3W_a^3)/W_H^3 + W^3W_H^3W_a^3 - 6W^6W_a^4 +$$
$$W^6W_a^6 - 12W^6W_b + 30W^6W_aW_b +$$
$$(3W^3W_aW_b)/W_H^3 + 3W^3W_H^3W_aW_b -$$
$$18W^6W_a^2W_b - 6W^6W_a^3W_b +$$
$$6W^6W_a^4W_b + 9W^6W_b^2 -$$
$$18W^6W_aW_b^2 + 3W^4W_a^2W_b^2 +$$
$$9W^6W_a^2W_b^2 + 4W^6W_b^3 +$$
$$(W^3W_b^3)/W_H^3 + W^3W_H^3W_b^3 -$$
$$6W^6W_aW_b^3 + 2W^6W_a^3W_b^3 -$$
$$6W^6W_b^4 + 6W^6W_aW_b^4 + W^6W_b^6, \qquad (4.3)$$

$$c_1 = W^2/W_H^2 - W^4/W_H^2 -$$
$$W/W_H - WW_H + W^2W_H^2 -$$
$$W^4W_H^2 + (W^4W_a)/W_H^2 + W^4W_H^2W_a +$$
$$(W^4W_a^2)/W_H^2 + W^4W_H^2W_a^2 -$$
$$(W^4W_a^3)/W_H^2 - W^4W_H^2W_a^3 +$$
$$(W^4W_b)/W_H^2 + W^4W_H^2W_b -$$
$$(W^2W_aW_b)/W_H^2 - (W^4W_aW_b)/W_H^2 +$$
$$(2W^3W_aW_b)/W_H - (2W^5W_aW_b)/W_H +$$
$$2W^3W_HW_aW_b - 2W^5W_HW_aW_b -$$
$$W^2W_H^2W_aW_b -$$
$$W^4W_H^2W_aW_b + (3W^5W_a^2W_b)/W_H +$$
$$3W^5W_HW_a^2W_b - (W^5W_a^4W_b)/W_H -$$
$$W^5W_HW_a^4W_b + (W^4W_b^2)/W_H^2 +$$
$$W^4W_H^2W_b^2 +$$
$$(3W^5W_aW_b^2)/W_H + 3W^5W_HW_aW_b^2 -$$
$$(3W^5W_a^2W_b^2)/W_H - 3W^5W_HW_a^2W_b^2 -$$
$$(W^4W_b^3)/W_H^2 - W^4W_H^2W_b^3 -$$
$$(W^5W_aW_b^4)/W_H - W^5W_HW_aW_b^4, \qquad (4.4)$$

$$c_2 = [W^3(1 + W_H^2)(-1 + W_a)(-1 + W_b)]/W_H, \quad (4.5)$$

$$c_3 = 2W^4(-1 + W_a)(-1 + W_b)(-1 +$$
$$W_a + W_b + W_aW_b), \qquad (4.6)$$

$$s_1 = -[W(-1 + W_H)(1 + W_H)(W -$$
$$W^3 + W_H + WW_H^2 - W^3W_H^2 +$$
$$W^3W_a + W^3W_H^2W_a + W^3W_a^2 +$$
$$W^3W_H^2W_a^2 - W^3W_a^3 - W^3W_H^2W_a^3 +$$
$$W^3W_b + W^3W_H^2W_b -$$
$$WW_aW_b - W^3W_aW_b -$$
$$2W^2W_HW_aW_b + 2W^4W_HW_aW_b -$$

$$WW_H^2W_aW_b - W^3W_H^2W_aW_b -$$
$$3W^4W_HW_a^2W_b + W^4W_HW_a^4W_b +$$
$$W^3W_b^2 + W^3W_H^2W_b^2 -$$
$$3W^4W_HW_aW_b^2 + 3W^4W_HW_a^2W_b^2 -$$
$$W^3W_b^3 - W^3W_H^2W_b^3 +$$
$$W^4W_HW_aW_b^4)]/W_H^2, \qquad (4.7)$$

$$s_2 = -[W^3(-1 + W_H)(1 + W_H)(-1$$
$$+ W_a)(-1 + W_b)]/W_H, \qquad (4.8)$$

$$s_4 = [W(-1 + W_H)(1 + W_H)(W -$$
$$W^3 + W_H + WW_H^2 - W^3W_H^2 +$$
$$W^3W_a + W^3W_H^2W_a +$$
$$W^3W_a^2 + W^3W_H^2W_a^2 -$$
$$W^3W_a^3 - W^3W_H^2W_a^3 +$$
$$W^3W_b + W^3W_H^2W_b -$$
$$WW_aW_b - W^3W_aW_b -$$
$$2W^2W_HW_aW_b + 2W^4W_HW_aW_b -$$
$$WW_H^2W_aW_b - W^3W_H^2W_aW_b -$$
$$3W^4W_HW_a^2W_b + W^4W_HW_a^4W_b +$$
$$W^3W_b^2 + W^3W_H^2W_b^2 -$$
$$3W^4W_HW_aW_b^2 + 3W^4W_HW_a^2W_b^2 -$$
$$W^3W_b^3 - W^3W_H^2W_b^3 +$$
$$W^4W_HW_aW_b^4)]/W_H^2. \qquad (4.9)$$

We substitute the D-function into (3.4) and solve them with respect to (ω_x, ω_y) as a function of θ. Substituting the solution $(\omega_x(\theta), \omega_y(\theta))$ into (3.5)–(3.8), we obtain the interface tension, 2D island shape and the interface stiffness.

Note that the D-function has the mirror symmetry with respect to k_x-axis, i. e. $D(k_x, k_y) = D(k_x, -k_y)$. Therefore, the island shape has the mirror symmetry with respect to k_x-axis. That is, $\omega_y(0) = 0$ and $\omega_y(\pi) = 0$ are the solutions of (3.4). At the orientation corresponding to $\theta = 0$ or $\theta = \pi$, the form (4.2) reduces to

$$D(k_x, 0) = M + c_3 + c_1 \cosh(k_x) +$$
$$2c_1 \cosh(k_x/2) + +c_2 \cosh(2k_x) +$$
$$2c_2 \cosh(k_x) + 2c_3 \cosh(3k_x/2) +$$
$$s_1 \sinh(k_x) + s_2 \sinh(2k_x) -$$
$$2s_2 \sinh(k_x) + 2s_4 \sinh(k_x/2). \qquad (4.10)$$

From the solution of $D(k_x, 0) = 0$ ($\omega_y(0) = \omega_y(\pi) = 0$), we obtain $\cosh(\omega_x(0)/2)$ and $\cosh(\omega_x(\pi)/2)$. Then, from (3.5), step tension becomes

$$\gamma(0) = 2k_\mathrm{B}T\cosh^{-1}(\omega_x(0)/2),$$
$$\gamma(\pi) = 2k_\mathrm{B}T\cosh^{-1}(\omega_x(\pi)/2). \qquad (4.11)$$

In the $T \to 0$ limit, step tensions (step free energy per lattice constant) becomes,

4

$$\gamma(0) = \mathrm{Min}[2J_1 + 4J_2 + \frac{2}{3}H,$$
$$2(2J_1 + 4J_2 - \frac{2}{3}H)],$$
$$\gamma(\pi) = \mathrm{Min}[2J_1 + 4J_2 - \frac{2}{3}H,$$
$$2(2J_1 + 4J_2 + \frac{2}{3}H)], \tag{4.12}$$

where $\mathrm{Min}[a,b]$ denotes the smaller one in $\{a,b\}$.

From (3.7), the step stiffness becomes,

$$\tilde\gamma(0) = k_B T[|c_1 \sinh(\omega_x(0)/2) +$$
$$(c_1 + 2c_2)\sinh(\omega_x(0)) +$$
$$3c_3 \sinh(3\omega_x(0)/2) + 2c_2 \sinh(2\omega_x(0)) +$$
$$s_4 \cosh(\omega_x(0)/2) + (s_1 + 2s_2)\cosh(\omega_x(0)) +$$
$$2s_2 \cosh(2\omega_x(0))|]/[2c_y^2(2c_3 +$$
$$c_1 \cosh(\omega_x(0)/2) + 4c_2 \cosh(\omega_x(0)) +$$
$$c_3 \cosh(3\omega_x(0)/2) + s_4 \sinh(\omega_x(0)/2) -$$
$$4s_2 \sinh(\omega_x(0)))], \tag{4.13}$$

$$\tilde\gamma(\pi) = k_B T[|c_1 \sinh(\omega_x(\pi)/2) +$$
$$(c_1 + 2c_2)\sinh(\omega_x(\pi)) +$$
$$3c_3 \sinh(3\omega_x(\pi)/2) + 2c_2 \sinh(2\omega_x(\pi)) +$$
$$s_4 \cosh(\omega_x(\pi)/2) + (s_1 + 2s_2)\cosh(\omega_x(\pi)) +$$
$$2s_2 \cosh(2\omega_x(\pi))|]/[2c_y^2(2c_3 +$$
$$c_1 \cosh(\omega_x(\pi)/2) + 4c_2 \cosh(\omega_x(\pi)) +$$
$$c_3 \cosh(3\omega_x(\pi)/2) + s_4 \sinh(\omega_x(\pi)/2) -$$
$$4s_2 \sinh(\omega_x(\pi)))]. \tag{4.14}$$

In Fig. 3, we show an example of equilibrium island shape and a polar graph of step stiffness at $J_1 = 165\mathrm{meV}$, $J_2/J_1 = -0.1$, lattice constant$= 3.84\text{Å}$ and $H/J_1 = 0.31$. We also show the temperature dependence of step tension, step stiffness, the coefficient of step interaction (3.11) where $g = B/a_h^3$, $a_h = 3.14\text{Å}$ and $g_0 = 0$.

In the absence of nnn interactions, W_a and W_b reduce to unity. The D-function (4.2), then, becomes

$$D(k_x, k_y) = M + c_1 \cosh(k_x) +$$
$$2c_1 \cosh(k_x/2 - c_y k_y) + c_1 \cosh(k_x/2 + c_y k_y) +$$
$$s_1 \sinh(k_x) + s_4 \sinh(k_x/2 - c_y k_y) +$$
$$s_4 \sinh(k_x/2 + c_y k_y), \tag{4.15}$$

$$M = 1 + 3W^2 + 3W^4 + W^6 + 4W^3(W_H^3 +$$
$$1/W_H^3),$$
$$c_1 = -(1 - W)^2 W(1 + W)^2(1 + W_H^2)/W_H,$$
$$s_1 = -s_4$$
$$= (1 - W)^2 W(1 + W)^2(1 + W_H)(1 -$$
$$W_H)/W_H,$$
$$c_2 = c_3 = s_2 = 0, \tag{4.16}$$

which agrees with the D-function given in Ref. [13].

B. The case of $H = 0$

At $H = 0$, s_1, s_2 and s_4 in (4.2) become zero, since W_H reduces to unity. The D-function, then, has the symmetry $D(k_x, k_y) = D(\pm k_x, \pm k_y)$. The island shape has the mirror symmetry with respect to the k_y-axis too; $\omega_x(\pi/2) = \omega_x(3\pi/2) = 0$ becomes the solution of (3.4). The equation

$$D(0, k_y) = M + c_1 + c_2 + 2(c_1 + c_3)\cosh(c_y k_y) +$$
$$(2c_2 + c_3)\cosh(2c_y k_y)$$
$$= 0, \tag{4.17}$$

is solved, in terms of $\cosh(c_y \omega_y)$ ($k_y = i\omega_y$), as

$$\cosh(c_y \omega_y) = -\frac{c_1 + c_3}{2(2c_2 + c_3)} +$$
$$\sqrt{\frac{(c_1 + c_3)^2}{4(2c_2 + c_3)^2} + \frac{-c_1 + c_2 + c_3 - M}{2(2c_2 + c_3)}}$$
$$\equiv z. \tag{4.18}$$

By use of this solution, we obtain step tension as

$$\gamma(\pi/2) = \gamma(3\pi/2)$$
$$= \frac{k_B T}{c_y} \cosh^{-1}(z), \tag{4.19}$$

and the step stiffness as

$$\tilde\gamma(\pi/2) = \tilde\gamma(3\pi/2)$$
$$= \frac{-4k_B T c_y \sqrt{z^2 - 1}|c_1 + c_3 + 2(2c_2 + c_3)z|}{2c_1 + 4c_2 + (c_1 + 9c_3)z + 8c_2 z^2}. \tag{4.20}$$

In the case of $J_{A2} = J_{B2} = 0$, the D-function reduces to that of the exact solution for the nn honeycomb lattice system [22].

That is,

$$D(k_x, k_y) = M + c_1 \cosh(k_x) + c_1 \cosh(k_x/2 - c_y k_y) +$$
$$c_1 \cosh(k_x/2 + c_y k_y),$$

$$M = (1 + W)^2(1 - 2W + 6W^2 -$$
$$2W^3 + W^4),$$
$$c_1 = -2(1 - W)^2 W(1 + W)^2,$$
$$c_2 = c_3 = s_1 = s_2 = s_4 = 0. \tag{4.21}$$

At $\theta = 0$, we obtain an explicit form of the solutions as

$$\omega_y(0) = 0,$$
$$\cosh(\omega_x(0)/2) = \frac{1}{2}\sqrt{3 - 2M/c_1} - \frac{1}{2}. \tag{4.22}$$

Also, at $\theta = \pi/2$, we have

$$\omega_x(\pi/2) = 0,$$
$$\cosh(c_y \omega_y(\pi/2)) = \frac{1}{2}(-M/c_1 - 1). \tag{4.23}$$

5

Hence, the interface tensions become

$$\gamma(0) = 2k_B T \ln(m_y),$$
$$m_y = -\frac{1}{2} + \frac{1}{2}z_2 + \frac{1}{2}\sqrt{(z_2 - 3)(z_2 + 1)},$$
$$z_2 = \frac{(1 + W)\sqrt{1 - W + W^2}}{\sqrt{W}|1 - W|} \tag{4.24}$$

$$\gamma(\pi/2) = 1/c_y \cdot k_B T \ln[(-2 + 1/W + W)/2]. \tag{4.25}$$

Due to the Wulff's theorem, $\gamma(0)$ and $\gamma(\pi/2)$ give the linear size of the island shape along x- and y-direction. The explicit form of interface stiffness becomes

$$\tilde{\gamma}(0) = \frac{k_B T}{c_y^2} \frac{z_2\sqrt{-3 - 2z_2 + z_2}}{2(z_2 - 1)} \tag{4.26}$$

$$\tilde{\gamma}(\pi/2) = 4k_B T c_y$$
$$\times \frac{(1 + W^2)|1 - 4W + W^2|}{1 + 4W - 6W^2 + 4W^3 + W^4}. \tag{4.27}$$

C. Triangular lattice

In the limit of $J_1 \to 0$, the system becomes two independent triangular lattice gases. In this case, the random walk treatment on the honeycomb lattice may not be good enough. In fact, (4.2) in this limit gives D-function slightly different from the known exact one on the triangular lattice. Hence, we need a separate study to treat this case.

The D-function of the triangular lattice becomes

$$D_3(k_x, k_y) = M - c_1 \cosh(k_y) - c_2 \cosh(\sqrt{3}k_x/2 - k_y/2) - c_3 \cosh(\sqrt{3}k_x/2 + k_y/2), \tag{4.28}$$

where

$$M = 1 + W_1^2 W_2^2 + W_1^2 W_3^2 + W_2^2 W_3^2,$$
$$c_1 = 2(1 - W_1)(1 + W_1)W_2 W_3,$$
$$c_2 = 2W_1 W_2(1 - W_3)(1 + W_3),$$
$$c_3 = 2W_1(1 - W_2)(1 + W_2)W_3, \tag{4.29}$$

$W_1 = \exp[-2J_1/(k_B T)]$, $W_2 = \exp[-2J_2/(k_B T)]$, and $W_3 = \exp[-2J_3/(k_B T)]$. The equations agree with the known exact one [22]. Note that the form of $D_3(k_x, k_y)$ (4.27) is essentially the same as $D(k_x, k_y)$ of nn honeycomb lattice (4.20). Therefore, the island shape of triangular lattice obtained from (3.4) is the same as the one of honeycomb lattice. The difference is the temperature dependence of coefficients. When $J_1 = J_2 = J_3 = J$, i.e., $W_1 = W_2 = W_3 = W$, D-function has a symmetry of $D_3(k_x, k_y) = D_3(\pm k_x, \pm k_y)$. Hence, we have explicit forms of γ and $\tilde{\gamma}$ for special orientations. Therefore, we have

$$\gamma_3(0) = \frac{2}{\sqrt{3}}k_B T \ln[\frac{1 - W^2}{2W^2}], \tag{4.30}$$
$$\gamma_3(\pi/2) = 2k_B T \times$$
$$\cosh^{-1}\left(-\frac{1}{2} + \frac{1}{2}\sqrt{3 + \frac{1 + 3W^4}{W^2(1 - W)(1 + W)}}\right). \tag{4.31}$$

The step stiffness is written as

$$\tilde{\gamma}_3(0) = \frac{2\sqrt{3}k_B T(1 + W^2)|1 - 3W^2|}{1 + 6W^2 - 3W^4} \tag{4.32}$$

$$\tilde{\gamma}_3(\pi/2) = \frac{2k_B T}{3} \times$$
$$\frac{\sqrt{(1 + 3W^2)(1 + 3W^4 - 2Wz_1 + 2W^3 z_1)}}{W(z_1 - W)|1 - W^2|},$$
$$z_1 = \sqrt{\frac{1 + 3W^2}{1 - W^2}}. \tag{4.33}$$

V. APPLICATION TO SI(111) SURFACE

A. The 7×7 reconstructed surface

At temperatures lower than the $7 \times 7 \leftrightarrow 1 \times 1$ transition temperature ($\sim$1130 K), Si(111) surface forms 7×7 reconstructed structure called DAS (dimer adatom stacking-fault) structure [23]. The unit cell of the DAS structure is divided into the faulted half (FH) and the unfaulted half (UH) [24], each of which forms a triangular lattice. It has been observed that the step structure is well described by the combination of the FH unit and UH unit [25]. We consider, therefore, a pair of triangular sublattices, where the one represents the FH lattice system, and the other represents the UH one. Consequently, the system becomes equivalent to a stoichiometrically binary lattice gas on a honeycomb lattice with nn interactions, where the inequivalent sites of the lattice gas model are coarse-grained representations of these two halves of the 7×7 unit cell. Therefore, we can use (4.15) and (4.16) to calculated step quantities. In Fig. 2, we regard closed circles as FH units, and open circles as UH units. We set lattice constant = 3.84×7 Å, and step height = 3.14Å. We introduce the step running direction angle θ so that a straight step with $\theta = 0$ corresponds to (11$\bar{2}$) step (Fig. 4).

In spite of the extensive experimental studies on Si(111)7×7 structure, the values of kink energy and step tension have not been settled yet. As one trial, we adopt the result of Eaglesham *et al.* [26] where step tension γ at 700 °C was obtained from the equilibrium crystal shape (ECS) of Si: $\gamma_{111} = 5.7 \times 10^{-11}$ J/m for (111) surface and $\gamma_{100} = 1.0 \times 10^{-11}$ J/m for (100) surface. Due to the 2×1 reconstruction, this value of γ_{100} corresponds to the mean value of the S_A-step tension and the S_B-step tension, and is consistent with the one calculated in our previous papers [4,15].

6

We choose kink energy so that the calculated mean value of step tension for $(2\bar{1}\bar{1})$ and $(\bar{2}11)$ at 700 °C reproduces the above mentioned value 5.7×10^{-11} J/m (= 36 meV/Å). In addition, the experimental observation of the island shape (and also the shape of spiral step) gives further information on the kink energy, due to the Wulff's theorem for 2D ECS. Let $h_{\boldsymbol{n}}$ be the distance between the center (= Wulff point) of the ECS (island shape, in our case) and the tangential line of the ECS at a position on the ECS curve, where $\boldsymbol{n}$ is the interface normal vector at the position. The Wulff's theorem states that the ratio $h_{\boldsymbol{n}}/\gamma_{\boldsymbol{n}}$ ($\gamma_{\boldsymbol{n}}$: interface tension, or step tension in our case) is $\boldsymbol{n}$-independent, leading to a relation $\gamma_{\boldsymbol{n}}/\gamma_{\boldsymbol{n}'} = h_{\boldsymbol{n}}/h_{\boldsymbol{n}'}$ for arbitrary $\boldsymbol{n}$ and $\boldsymbol{n}'$. From the photographs of the experimental observation [27,28], we have $h_{\bar{2}11}/h_{2\bar{1}\bar{1}} = 1.2$. This ratio gives the ratio between the step free energies corresponding to these directions. At such low temperature where the observation was made, these step free energies are well approximated by the step formation energies $(2J + 2H/3)$ and $(2J - 2H/3)$ (see (4.12)), giving us $h_{\bar{2}11}/h_{2\bar{1}\bar{1}} = 1.2 = (2J + 2H/3)/(2J - 2H/3)$ which amounts to $H/J = 0.31$.

We then set $J = 0.475$eV and $H = 0.15$eV. The kink energy becomes 1.05eV$= 2J + 2H/3$ for $(2\bar{1}\bar{1})$ step and 0.85eV$= 2J - 2H/3$ for $(\bar{2}11)$ step, which are smaller than but is in the same order of magnitude of the ones reported in Refs. [29,21].

The difference in the on-site energy between the UH and FH, is then $E_{FH} - E_{UH} = 4H = 0.59$eV. In the first principles study of Meade and Vanderbilt [30], surface energies of the Si(111) surface for various structures are calculated: For example, 1.24 eV$/1 \times 1$ for the 2×2-adatom structure, and 1.27 eV$/1 \times 1$ for the 2×2-adatom (faulted) structure. From these values, we can estimate $E_{FH} - E_{UH}$ to be $(1.27 - 1.24) \times 24 \sim 0.7$eV which is in reasonable agreement with our value 0.59eV.

In Fig. 5, we show equilibrium island shape at 400 °C and 850 °C, and the temperature dependence of step tension, step stiffness and step interaction coefficient $g = B/a_h^3$ (see (3.11)). The step tension is almost constant below 1130K, because the temperature is very low as compared with the lattice-gas melting temperature of the model (~ 8300K). On the other hand, the step stiffness strongly depends on temperature in the same region. The step stiffness for $(2\bar{1}\bar{1})$ step increases rapidly as temperature decreases. While, the step stiffness of $(0\bar{1}1)$ step becomes smaller and smaller and converges to zero at zero temperature.

Note that a similar analysis can be made for $n \times n$ DAS structure. From the photographs of small island of 5×5 structure [28], we find that the island shape has a six-fold rotational symmetry in contrast to the case of the 7×7 structure which has a three-fold rotational symmetry. Recall that the six-fold rotational symmetry appear only when $H = 0$ (see §4.2). Therefore, the energy difference between FH and UH units in the case of 5×5 DAS structure is very small if exists. We stress here that, also

for other structures, observation of the anisotropy of the equilibrium island shape will be useful in determining the energy difference between FH and UH units.

B. The 1×1 high temperature surface

The high-temperature Si(111) surface at about 900 °C has the structure of the 1×1 surface together with disordered adatoms with concentration of 0.25 [31–33]. Further, Khomoto and Ichimiya [31] reported that the number ratio of adatoms sitting on T_4 site and H_3 site is 4:1. Although the adatoms are considered to be in a disordered phase, the broad $\sqrt{3} \times \sqrt{3}$ peaks appear in diffraction observations [34,31] which suggests existence of the short-range order corresponding to formation of the hard-hexagon units [35].

For the high temperature surface of Si(111), experimental measurement of the step tension and the step stiffness has been a subject of active study [21,36–39]. The experimental values are, however, not settled yet. We make, therefore, several trial calculations for possible cases. In all the cases, we choose the microscopic coupling constants so that the calculated step stiffness at 900°C reproduces the value presented by Bartelt *et al.* [36].

1. Case 1: Adatom in disordered phase without short-range order

We use the honeycomb lattice gas system of (4.2), with J_1 and J_2 being regarded as effective coupling constants.

In Fig. 2 we regard the filled circles as atoms of the top layer and the open circles as those of the second layer (the lattice constant = 3.84Å, the step height $a_h = 3.14$Å).

We introduce the step running direction angle θ so that a straight step with $\theta = 0$ corresponds to $(\bar{1}\bar{1}2)$ step. The effect of dangling bonds normal to (111) plane are taken into account by setting $H/J_1 = 1$.

We calculate equilibrium island shape, step stiffness and step interaction coefficient, which we show in Fig. 6. Here, assuming that J_2 is small, we have set $J_2/J_1 = 0.2$ and $J_1 = 60$meV. The kink energy becomes 176meV for $(2\bar{1}\bar{1})$ step and 256meV for $(\bar{2}11)$ step. As is seen in the island shape and the polar graph of step stiffness at 900°C, there remains anisotropy in the step stiffness in spite of the circular island shape. The most significant characteristic of this results is the asymmetry between the orientations $(2\bar{1}\bar{1})$ and $(\bar{2}11)$. In contrast to the 7×7 structure, the stiffness as a function of the step orientation takes its maximum at $(\bar{2}11)$.

2. Case 2: The $\sqrt{3} \times \sqrt{3}$ short-range ordered phase

In the case of $\sqrt{3} \times \sqrt{3}$-ordered phase of adatoms, we calculate step quantities by using the triangular lattice gas model (Fig. 7a). As has been pointed out in Sec. 4, the system has six-fold rotational symmetry. We set the lattice constant to be $3.84 \times \sqrt{3}$Å, and the step height to be 3.14Å. We introduce the step running direction angle θ so that a straight step with $\theta = 0$ corresponds to $(\bar{1}\bar{1}2)$ step. The step tension and the step stiffness are calculated exactly from (4.30)–(4.33). The effective coupling constant is obtained to be $J = 62$meV (kink energy = 248meV). We show the calculated results in Fig. 8. The step stiffness takes its maximum at the orientation $\{10\bar{1}\}$.

3. Case 3: The 2×2 short-range ordered phase

Calculation of step quantities can be done in the same fashion as in the case 2. We set the lattice constant as 3.84×2Å, and the step height as 3.14Å (Fig. 7b). We introduce the step running direction angle θ so that a straight step with $\theta = 0$ corresponds to $(0\bar{1}1)$ step. The step stiffness takes its maximum at $\{\bar{2}11\}$. The effective coupling constant is obtained to be $J = 67$meV (kink energy = 268meV). We show the calculated results in Fig. 9.

VI. SUMMARY

We have considered the honeycomb lattice Ising system in a staggered field with both nearest-neighbor (nn) and next-nearest-neighbor (nnn) interactions, to calculate interface tension, interface stiffness, island shape by the imaginary path-weight (IPW) method.

We have applied the calculated results to Si(111) 7×7-reconstructed surfaces and the high-temperature Si(111) 1×1 surface. We have made estimation on the microscopic coupling constants from existing experimental data, and have drawn equilibrium island shape, step tension, step stiffness and the coefficient of step interaction, with their temperature dependence. Our analysis made in the present paper will be helpful in determining precise value of the kink energy from experimental observation.

Our lattice-gas treatment made in the present paper corresponds to the two-level approximation for the surface fluctuation. Fortunately, the temperature-range of our concern in the present study is very low, the two-level approximation is expected to be fairly reliable. On the other hand, at higher temperatures, near the roughening transition temperature, we should consider multilevel fluctuation of the surface. Even in such cases, we have an efficient method, namely, the *temperature-rescaled Ising-model approach*, [15] where the IPW method is combined with the numerical renormalization-group method; [40] details will be discussed elsewhere.

[1] G. Binnig, H. Rohrer, Ch. Gerber and E. Weibel, Phys. Rev. Lett. **49** 120 (1983).
[2] E. Bauer, Ultramicroscopy **17** 57 (1985); E. Bauer and W. Telieps, Scanning Microscopy, Suppl. 1, 99 (1987); in *the Study of Surfaces and Interfaces by Electon Optical Techniques*, Eds. A. Howie and U. Valderé, p. 195 (Plenum, New York, 1988).
[3] K. Yagi, J. Appl. Cryst. **20** 147 (1987); N. Inoue, Y. Tanishiro and K. Yagi, Jpn. J. Appl. Phys. **26**, L293 (1987); T. Nakayama, Y. Tanishiro and K. Takayanagi, Jpn. J. Appl. Phys. **26**, L1186 (1987).
[4] N. Akutsu and Y. Akutsu, Surf. Sci. **376**, 92 (1997).
[5] N. V. Vdovichenko, Zh. Eksp. Theor. Fiz. **47**, 715 (1964) [Sov. Phys. JETP **20**, 477 (1965)]; R. P. Feynman, *Statistical Mechanics* (Benjamin/Cummings, Reading, Mass., 1972).
[6] M. Holzer, Phys. Rev. Lett. **64**, 653 (1990); Phys. Rev. B**42**, 10570 (1990).
[7] Y. Akutsu and N. Akutsu, Phys. Rev. Lett. **64**, 1189 (1990).
[8] N. Akutsu and Y. Akutsu, J. Phys. Soc. Jpn. **59**, 3041 (1990).
[9] B. S. Swartzentruber, Y.-W. Mo, R. Kariotis, M. G. Lagally, and M. B. Webb, Phys. Rev. Lett. **65**, 1913 (1990); B. S. Swartzentruber and M.Schacht, Surf. Sci. **322**, 83 (1995).
[10] N. C. Bartelt, R. M. Tromp, and E. D. Williams, Phys. Rev. Lett. **73**, 1656 (1994).
[11] R. K. P. Zia, Phys. Lett. **64**A, 345 (1978).
[12] D. B. Abraham, *Phase Transitions and Critical Phenomena*, Vol. 10, ed. C. Domb and J. L. Lebowitz, p. 1 (New York, Academic 1986).
[13] N. Akutsu, J. Phys. Soc. Jpn. **61**, 477 (1992).
[14] N. Akutsu and Y. Akutsu, J. Phys. Soc. Jpn. **64**, 736 (1995).

[15] N. Akutsu and Y. Akutsu, Phys. Rev. **B57**, R4233 (1998).

[16] A. F. Andreev, Zh. Eksp. Theor. Fiz. **80**, 2042 (1981) [Sov. Phys. JETP **53**, 1063 (1982)].

[17] E. E. Gruber and W. W. Mullins, J. Phys. Chem. Solids **28**, 6549 (1967); V. L. Pokrovsky and A. L. Talapov, Phys. Rev. Lett. **42**, 65 (1979) [Sov. Phys. JETP **51**, 134 (1980)].

[18] Y. Akustu, N. Akutsu and T. Yamamoto, Phys. Rev. Lett. **61**, 424 (1988).

[19] T. Yamamoto, Y. Akutsu and N. Akutsu, J. Phys. Soc. Jpn. **57**, 453 (1988).

[20] T. Yamamoto, Y. Akutsu and N. Akutsu, J. Phys. Soc. Jpn. **63** 915 (1994).

[21] E. D. Williams, R. J. Phaneuf, J. Wei, N. C. Bartelt and T. L. Einstein, Surf. Sci. **294**, 219 (1993); *ibid.* Surf. Sci. **310**, 451 (1994).

[22] R. K. P. Zia, J. Stat. Phys. **45**, 801 (1986).

[23] K. Takayanagi, Y. Tanishiro, S. Takahashi and M. Takahashi, J. Vac. Sci. Technol. A**3**, 1502 (1985).

[24] H. Neddermeyer, Rep. Prog. Phys. **59**, 701 (1996).

[25] H. Tochihara, W. Shimada, M. Itoh, H. Tanaka, M. Udagawa and I. Sumita, Phys. Rev. B**45**, 11332 (1992); K. Miki, Y. Morita, H. Tokumoto, T. Sato, M. Iwatsuki, M. Suzuki and T. Fukuda, Ultramicroscopy **42**-**44**, 851 (1992).

[26] D. J. Eaglesham, A. E. White, L. D. Feldman, N. Moriya and D. C. Jacobson, Phys. Rev. Lett. **70**, 1643 (1993).

[27] K. Yagi, A. Yamanaka, H. Sato, M. Shima, H. Ohse, S. Ozawa and Y. Tanishiro, Prog. Theor. Phys. Suppl. **106**, 303 (1991).

[28] A. Ichimiya, H. Nakahara, and Y. Tanaka, Thin solid Films **281**-**282**, 1 (1996); *ibid.* J. Cryst. Growth, **163**, 39 (1996).

[29] G. Wilhelmi, T. Kampschulte and H. Neddermeyer, Surf. Sci. **331**-**333**, 1408 (1995).

[30] R. D. Meade and D. Vanderbilt, Phys. Rev. B**40**, 3905 (1989).

[31] S. Kohmoto and A. Ichimiya, Surf. Sci. **223**, 400 (1989).

[32] A. V. Latyshev, A. B. Krasilnikov, A. L. Aseev, L. V. Sokolov and S. I. Stenin, Surf. Sci. **254**, 90 (1991).

[33] Y. -N. Yang and E. D. Williams, Phys. Rev. Lett. **72**, 1862 (1994).

[34] S. Ino, J. J. Appl. Phys. **16**, 891 (1977);
H. Iwasaki, S. Hasegawa, M. Akizumi, S.-Te Li, S, Nakamura and J. Kanamori, J. Phys. Soc. Jpn. **56**, 3425 (1987).

[35] Y. Sakamoto and J. Kanamori, J. Phys. Soc. Jpn. **58**, 2083 (1989).

[36] N. C. Bartelt, J. L. Goldberg, T. L. Einstein, E. D. Williams, J. C. Heyraud, and J. J. Métois, Phys. Rev. B**48**, 15453 (1993).

[37] Alfonso, J. C. Heyraud, and J. J. Métois, Surf. Sci. **291** (1993) L745; J. M. Bermond, J. J. Métois, J. C. Heyraud, and C. Alfonso, Surf. Sci. **331**-**333**, 855 (1995).

[38] M. Bermond, J. J. Métois, X. Egea, and F. Floret, Surf. Sci. **330**, 48 (1995); T. Suzuki, J. J. Métois and K. Yagi, Surf. Sci. **339**, 105 (1995).

[39] A.V. Latyshev, H. Minoda, Y. Tanishiro, and K. Yagi, Phys. Rev. Lett. **76**, 94 (1996); A. B. Latyshev, A. L. Aseev, A. B. Krasilnikov and S. I. Stenin, Surf. Sci **213**, 157 (1989); J. J. Métois and M. Audiffren, Int. J. Mod. Phys. B**11**, 3691 (1997).

[40] S. R. White, Phys. Rev. Lett. **69**, 2863 (1992); T. Nishino, J. Phys. Soc. Jpn. **64**, 3598 (1995); T. Nishino and K. Okunishi, J. Phys. Soc. Jpn. **64**, 4084 (1995).

FIG. 1.   Examples of an interface of square lattice Ising model made by fixing the boundary spins.

FIG. 2.   Examples of an interface configuration. A-atom and B-atom are indicated by filled circle and open circle, respectively. Thick line represents an interface.

FIG. 3.   An example of calculation by the use of the D-function of (4.2). (a) The island shape at $900°C$, (b) a polar graph of step stiffness at $900°C$, (c) temperature dependence of step tension, (d) temperature dependence of step stiffness, and (e) temperature dependence of $g = B/a_h^3$. We have set $J_1 = 165$meV, $J_2 = -16.5$mev, and $H = 165$meV: Kink energies are 88meV for $(2\bar{1}\bar{1})$ step and 176meV for $(\bar{2}11)$ step. In (c)-(e), thick lines correspond to$(\bar{2}11)$ step, thin lines to $(2\bar{1}\bar{1})$ step and broken lines to $\{10\bar{1}\}$ step.

FIG. 4.   Examples of a step edge on 7×7 reconstructed Si(111) surface. "U" denotes unfaulted half unit, and "F" denotes faulted half unit.

FIG. 5.   Calculation for 7×7 reconstructed surface by the use of the D-function of (4.15). (a) The island shape at $850°C$, (b) the island shape at $400°C$, (c) temperature dependence of step tension, (d) temperature dependence of step stiffness and (e) temperature dependence of $g = B/a_h^3$. We have set $J = 0.475$eV, $4H = 0.59$eV: Kink energy = 1.05eV for $(2\bar{1}\bar{1})$ step and 0.85eV for $(\bar{2}11)$ step. In (c)-(e), thick lines corresponds to $(2\bar{1}\bar{1})$ step, thin lines to $(\bar{2}11)$step and broken lines to $\{10\bar{1}\}$ step.

FIG. 6.   Calculation for 1×1 surface (Case 1) by the use of D-function of (4.2). (a) The island shape at $900°C$, (b) a polar graph of step stiffness at $900°C$, (c) temperature dependence of step tension, (d) temperature dependence of step stiffness and (e) temperature dependence of $g = B/a_h^3$. We have set $J_1 = 60$meV,$J_2 = 12$mev, and $H = 60$meV: Kink energy = 176meV for $(2\bar{1}\bar{1})$ step and 256meV for $(\bar{2}11)$ step. In (c)-(e), thick lines corresponds to $(2\bar{1}\bar{1})$ step, thin lines to $(\bar{2}11)$step and broken lines to $\{10\bar{1}\}$ step. Open squares: Ref. [37]. Open circle: Ref. [35].

FIG. 7.　Examples of an interface configuration for two cases of adatom orderings: (a) $\sqrt{3} \times \sqrt{3}$ and (b) 2×2. Thick line represents the interface. A-atom and B-atom are indicated by filled circle and open circle, respectively. Adatoms are indicated by shaded large circles. Broken lines denote boundaries between the hexagons.

FIG. 8.　Case 2. Calculation for $\sqrt{3} \times \sqrt{3}$ adatom ordering (Case 2) by the use of D-function of (4.30)–(4.33). (a) The island shape at $900°$C, (b) a polar graph of step stiffness at $900°$C, (c) temperature dependence of step tension, (d) temperature dependence of step stiffness, (e) temperature dependence of $g = B/a_h^3$. We have set $J = 62$meV: Kink energy $= 248$meV for $\{10\bar{1}\}$ step. In (c)-(e), thick lines corresponds to $\{2\bar{1}\bar{1}\}$ step and thin lines to $\{10\bar{1}\}$ step. Open squares: Ref. [37]. The open circle: Ref. [35].

FIG. 9.　Case 3. Calculation for 2×2 adatom ordering (Case 3) by the use of D-function of (4.30)–(4.33). (a) The island shape at $900°$C, (b) a polar graph of step stiffness at $900°$C, (c) temperature dependence of step tension, (d) temperature dependence of step stiffness and (e) temperature dependence of $g = B/a_h^3$. We have set $J = 67$meV: Kink energy $= 268$meV for $2\bar{1}\bar{1}$ step. In (c)-(e), thick lines correspond to $\{2\bar{1}\bar{1}\}$ step and thin lines to $\{10\bar{1}\}$ step. Open squares: Ref. [37]. The open circle: Ref. [35].
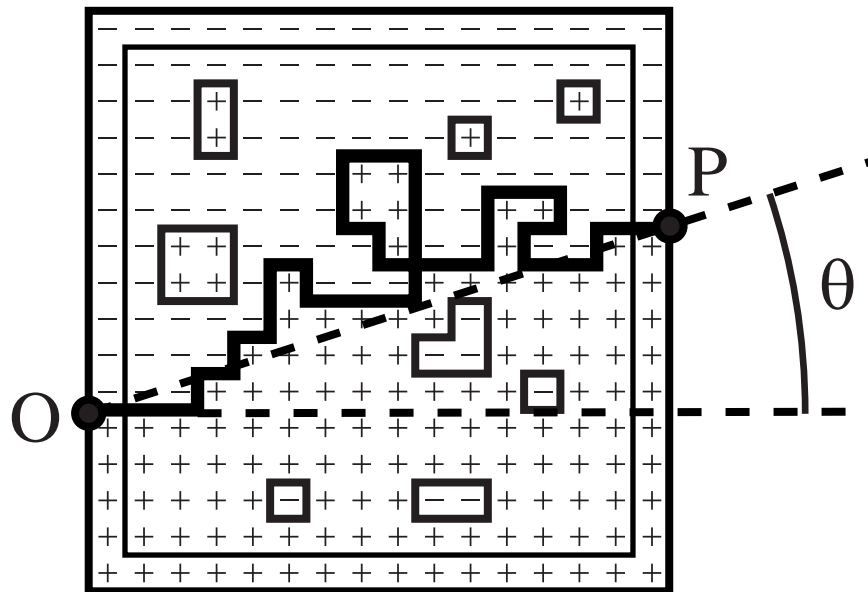
Figure 1   N. Akutsu and Y. Akutsu
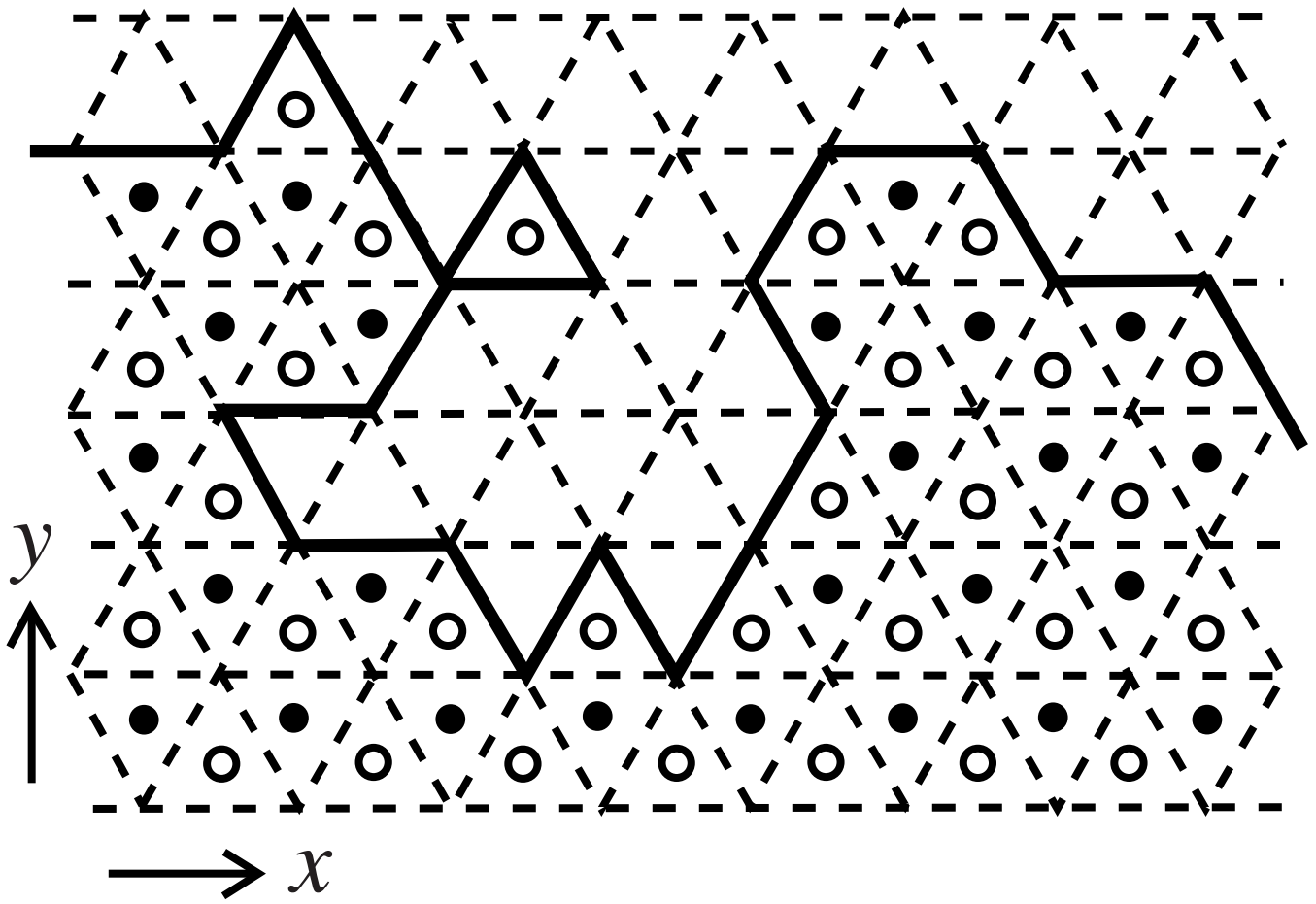
Figure 2   N. Akutsu and Y. Akutsu

(a)

[1̄1̄2]

[11̄2̄1]

900°C

0.3
0.2
0.1
-0.3 -0.2 -0.1   0.1 0.2 0.3
-0.1
-0.2
-0.3

(b)

γ̃

[1̄1̄2]

[11̄2̄1]

900°C

0.6
0.4
0.2
-0.6 -0.4 -0.2   0.2 0.4 0.6
-0.2
-0.4
-0.6

(meV/Å)

(c)

50
40
30
20
10
0

γ

0 200 400 600 800 1000 1200 1400 1600
T   (K)

(meV/Å)

(d)

50
40
30
20
10
0

γ̃

0 200 400 600 800 1000 1200 1400 1600
T   (K)

(meV/Å²)

(e)

250
200
150
100
50
0

g

800   1000   1200   1400   1600
T   (K)
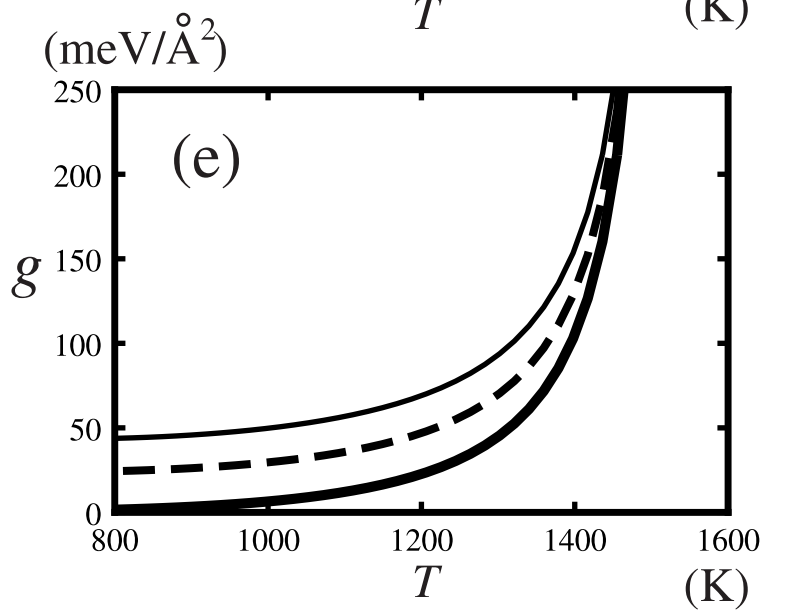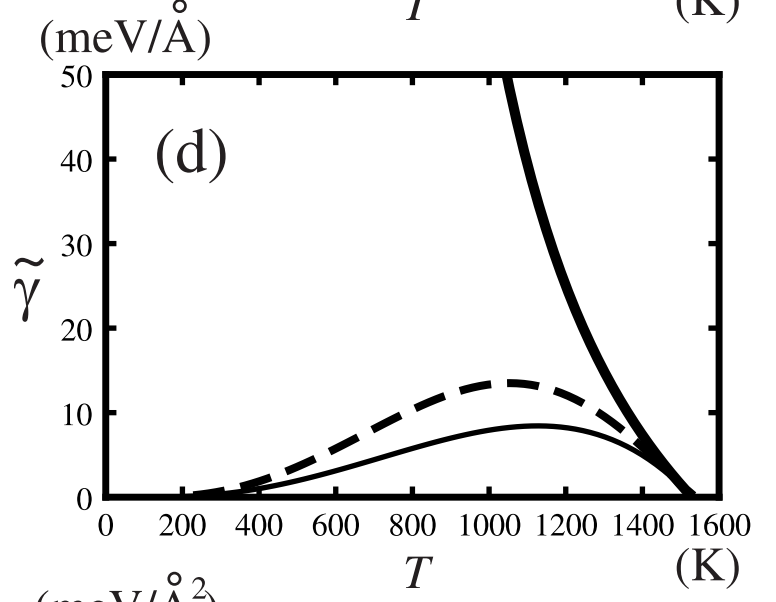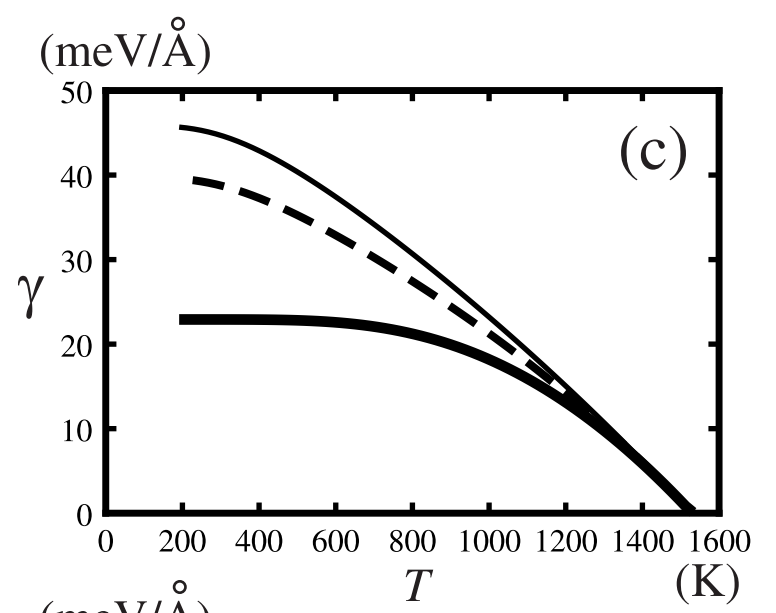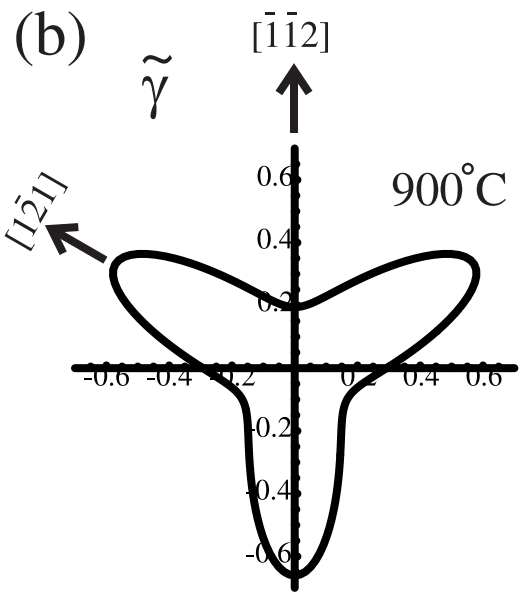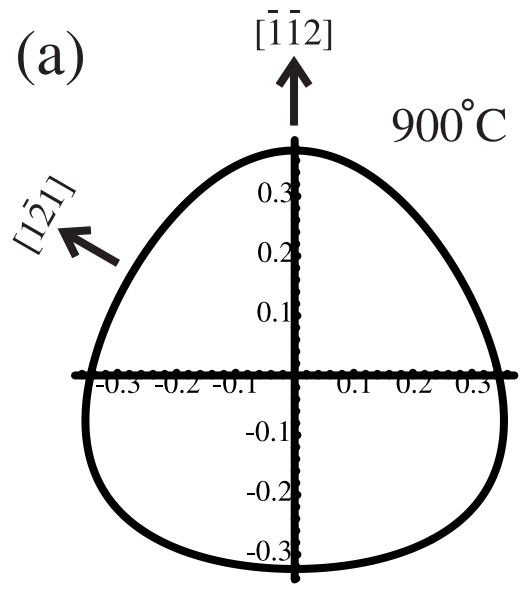
Figure 3   N. Akutsu and Y. Akutsu

$[11\bar{2}]$
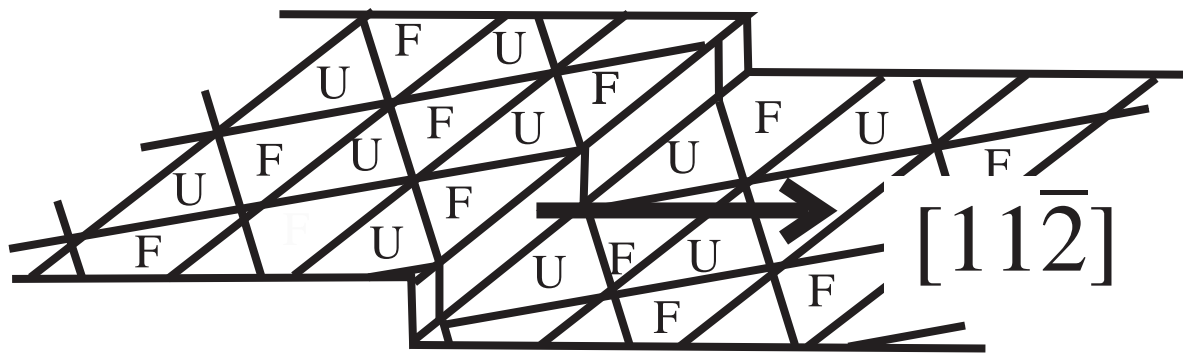
Figure 4   N. Akutsu and Y. Akutsu

(a)

850 °C

[11$\bar{2}$]

[$\bar{1}$2$\bar{1}$]

(c)

(meV/Å)

γ

T (K)

(b)

400°C

[11$\bar{2}$]

[$\bar{1}$2$\bar{1}$]

(d)

(meV/Å)

$\tilde{\gamma}$

T (K)

(e)

(meV/Å^2)

g

T (K)
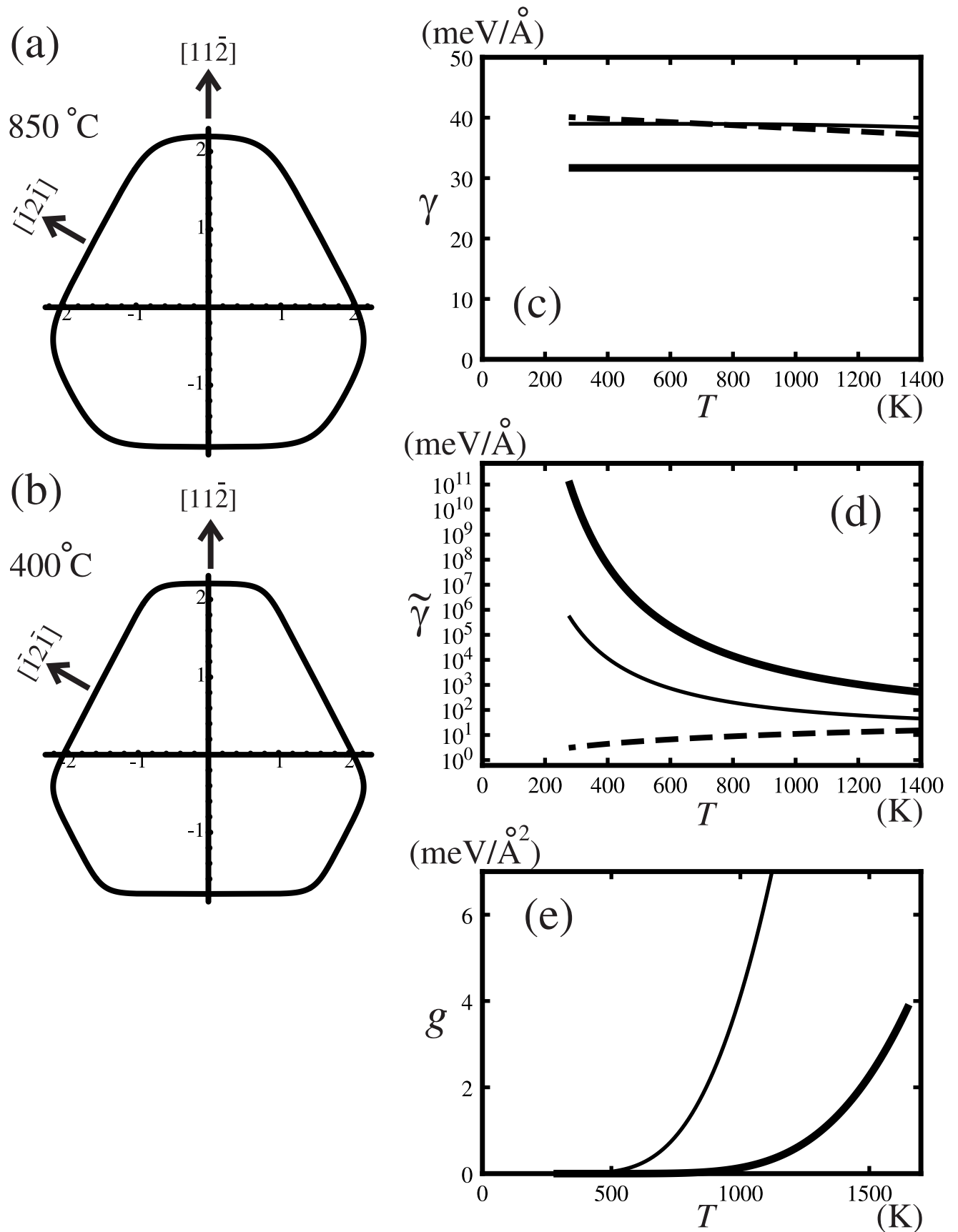
Figure 5   N. Akutsu and Y. Akutsu
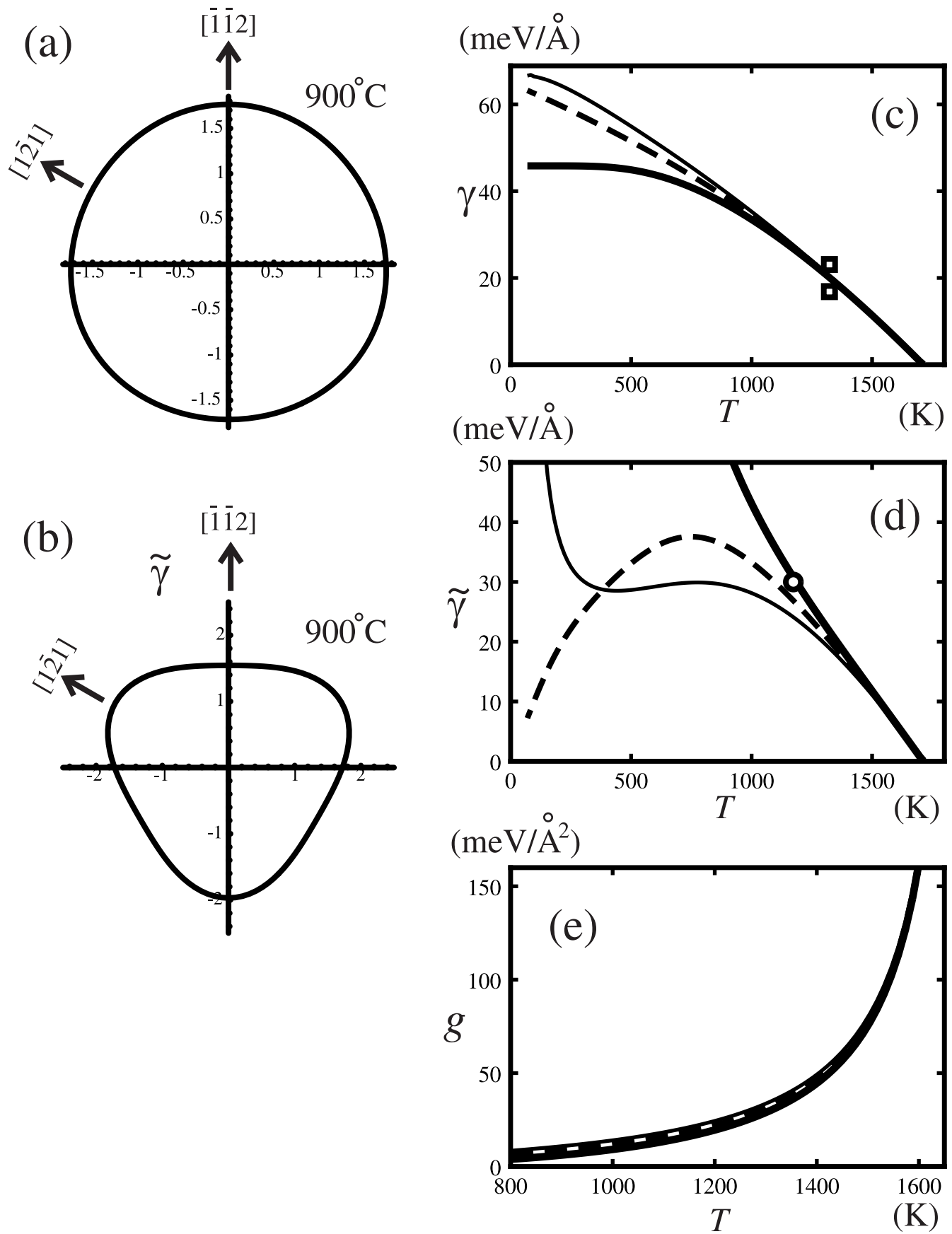
Figure 6   N. Akutsu and Y. Akutsu
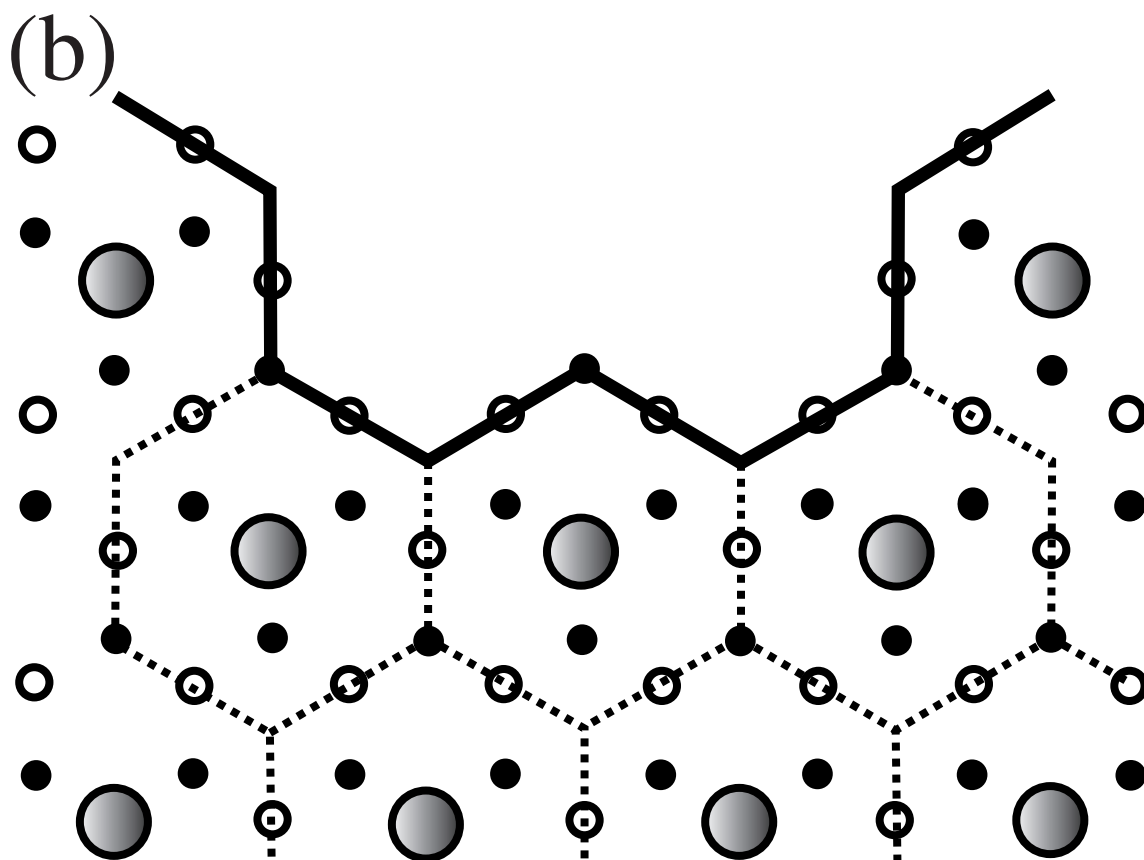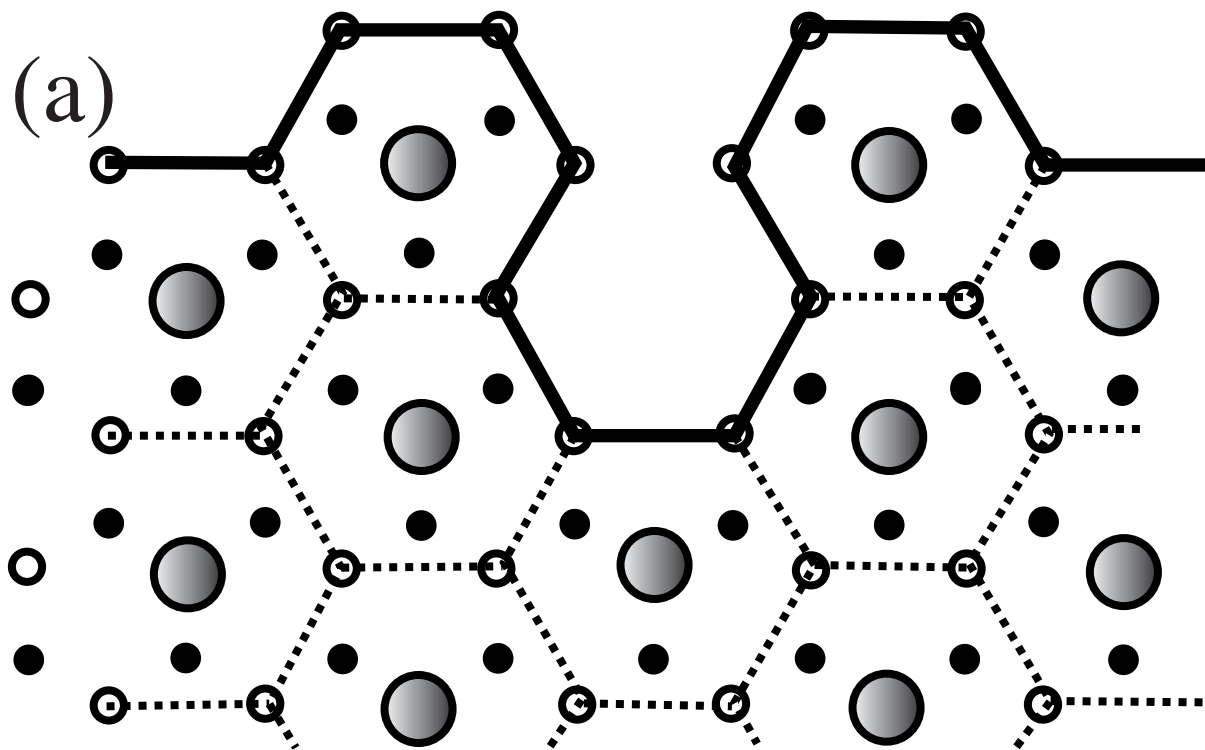
Figure 7   N. Akutsu and Y. Akutsu
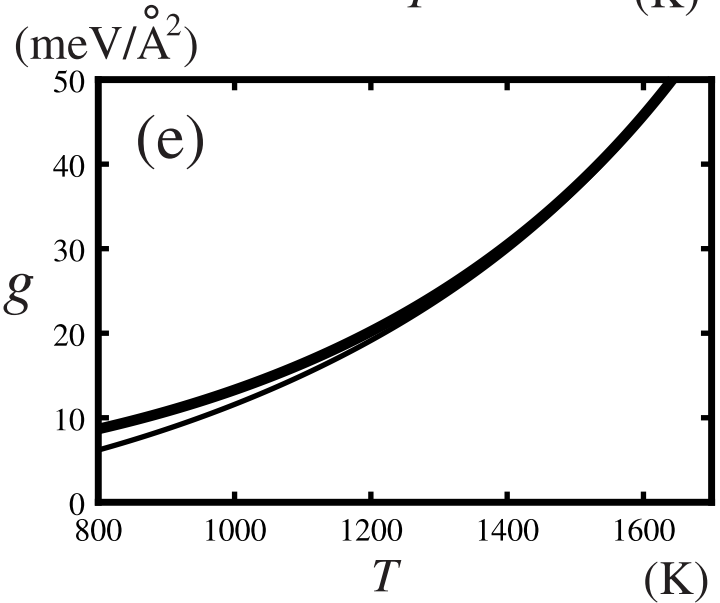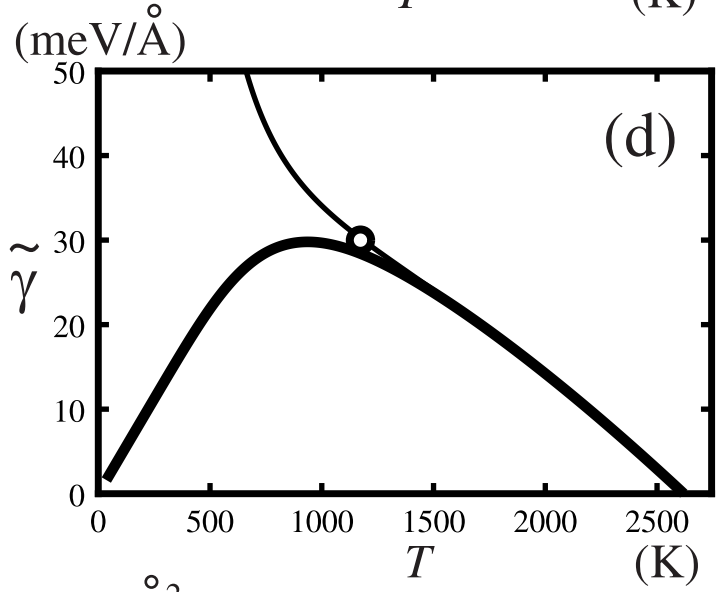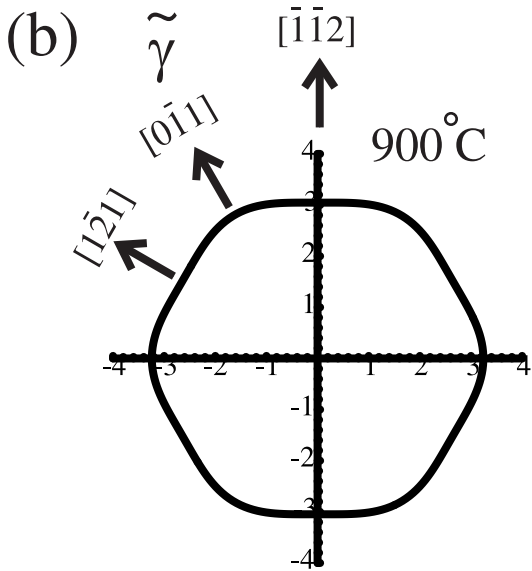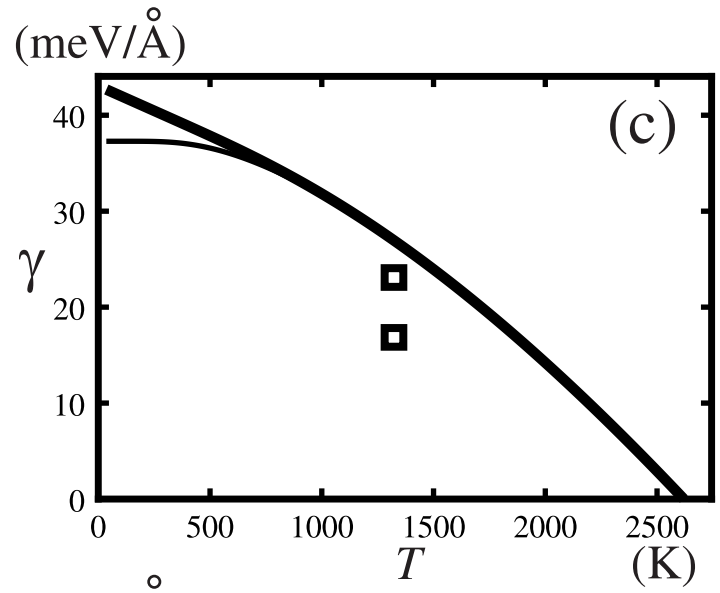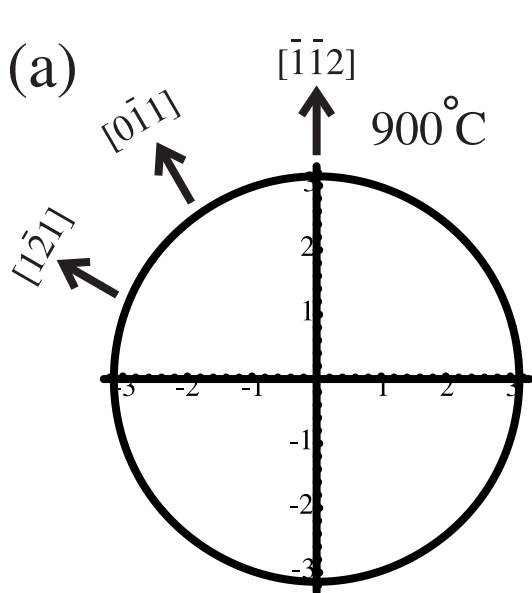
Figure 8   N. Akutsu and Y. Akutsu
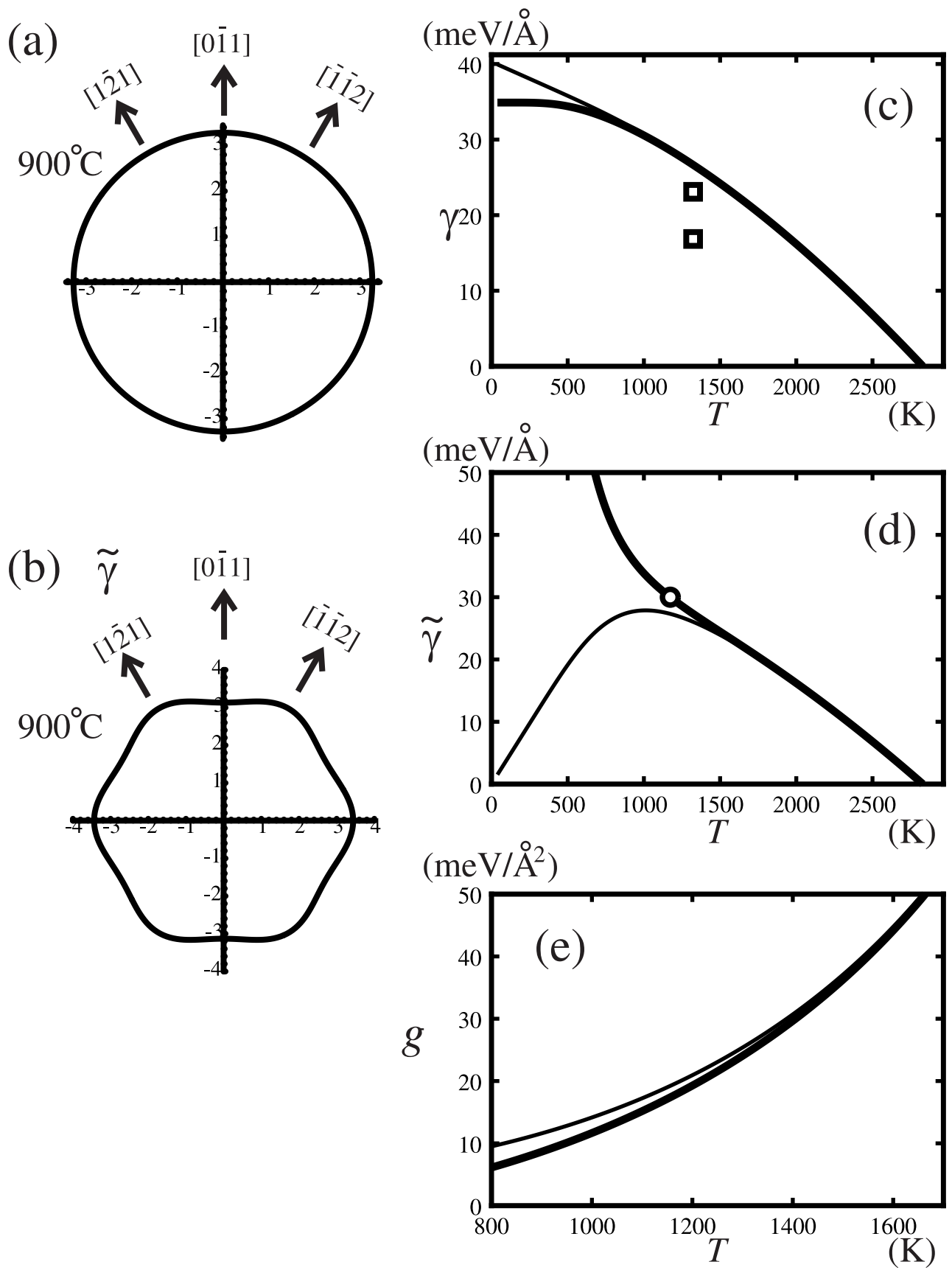
Figure 9   N. Akutsu and Y. Akutsu